Title: A dopamine-dependent mechanism for reward-induced modification of fear memories

Authors: Mi-Seon Kong[1#], Yong S. Jo[2#], Ekayana Sethi[1], Gyeong Hee Pyeon[2] and Larry S. Zweifel[1,3]

# These authors contributed equally to this work.

Affiliations: 1. Department of Psychiatry and Behavioral Sciences, University of Washington, Seattle WA USA. 2. School of Psychology, Korea University, Seoul, Republic of Korea. 3. Department of Pharmacology, University of Washington, Seattle WA USA.

Corresponding authors: larryz@uw.edu and ysjo@korea.ac.kr

Abstract

A positive mental state has been shown to modulate fear-related emotions associated with the recall of fear memories. These, and other observations suggest the presence of central brain mechanisms for affective states to interact. The neurotransmitter dopamine is important for both reward- and fear-related processes, but it is unclear whether dopamine contributes to such affective interactions. Here, we show that precisely timed reward-induced activation of dopamine neurons in mice potently modifies fear memories and enhances their extinction. This reward-based switch in fear states is associated with changes in dopamine release and dopamine-dependent regulation of fear encoding in the central amygdala (CeA). These data provide a central mechanism for reward-induced modification of fear states that have broad implications for treating generalized fear disorders.

Summary

Reward-induced dopamine release in the central amygdala switches fear states and modifies fear encoding.

Main text:

In human subjects, positive emotions have been shown to have an inhibitory effect on fear generalization (*1*). Positive affect has also been shown to enhance the extinction of fear memories (*2*). However, it is currently unclear the extent to which positive reward-associated memories can modify fear memories or how this occurs at the level of brain circuitry. Based on their roles in regulating behavioral responses to both positive and negative affective stimuli (*3-6*), and the numerous connections between them (*7-10*), we hypothesized that ventral tegmental area (VTA) dopamine-releasing neurons and GABA-releasing neurons of the CeA may be central to the mechanism of positive reinforcement induced suppression of fear states.

Reward and fear-associated stimuli increase the activity of VTA dopamine neurons (*11, 12*). However, during intense threat or increasing threat uncertainty dopamine neuron activity is diminished and fear generalization occurs in a manner that is dependent on the CeA (*7*). To determine the extent to which a positive affective memory can impact fear memories and the dopamine dependence of such modifications, we asked whether recall of a reward associated stimulus (reward conditioned stimulus, CS_{Rew+}) could modify fear states under different conditions by increasing dopamine neuron activity. To achieve this, recall of a CS_{Rew+} memory was precisely timed with delivery of a fear conditioned stimulus (CS_{Fear+}). For reward conditioning, we utilized a Pavlovian reward reinforcement task (**fig. S1A**) in which a 10s tone (CS_{Rew}+) co-terminates with the delivery of a food reinforcer (reward US, 25-CS/US pairings). As a control, a second tone was played (10s) an equal number of times but not paired with reward delivery (CS_{Rew}-). During the positive reinforcement task, mice learned to discriminate between the CS_{Rew}+ and CS_{Rew}- (**fig. S1B**) and dopamine neuron activity (**fig. S1C-H**) displayed increased conditioned responses to the CS_{Rew}+ (**Fig. 1A**) that coincided with reduced responding

to the reward US (Reward) (**Fig. 1A,B**), as predicted (*11*). Next, mice underwent Pavlovian discriminatory fear conditioning following positive reinforcement learning (**Fig. 1C** and **fig. S2A-E**) using a high intensity foot shock ($US_{0.5mA}$) to induce generalized threat responses (*7*). In the control group, mice were presented with the CS_{Rew}- for 1s at the onset of the CS_{Fear}+ (10s tone) and in the experimental group mice were presented with the CS_{Rew}+ to invoke increased dopamine neuron activity at the onset of the CS_{Fear}+ (**Fig. 1C** and **fig. S2A**). In a separate group of mice, VTA dopamine neurons were inhibited during the 1s of CS_{Rew}+ presentation (JAWS-CS_{Rew}+) (*13*) to establish the activity dependence of these cells (**Fig. 1C** and **fig. S2A-C**). Following positive reinforcement learning (**fig. S2D**), mice presented with the CS_{Rew}- at the onset of the CS_{Fear}+ displayed generalized fear (**Fig 1D**); however, mice presented with the CS_{Rew}+ displayed discriminatory fear responses (**Fig 1D**), an effect that was blocked by inhibition of dopamine neurons (**Fig. 1D** and **fig. S2F**).

Like high intensity threats, increased uncertainty in the delivery of a lower intensity foot shock ($US_{0.3mA}$) promotes generalized fear (*7, 14*). To determine whether a positive stimulus can prevent generalization associated with uncertainty, mice were conditioned in a probabilistic conditioning paradigm (**fig. S3A**) (*7, 15*). Brief co-presentation of the CS_{Rew}+, but not the CS_{Rew}-, with the higher probability fear CS ($CS_{0.7}$), promoted discriminatory fear learning that was blocked with inhibition of VTA dopamine neurons during the CS_{Rew}+ presentation (**fig. S3A-D**). Thus, the recall of a positive memory can modify generalized fear memories that are generated under different conditions.

During fear extinction training, dopamine neurons that are inhibited by the CS_{Fear}+ are activated by the omission of the predicted US_{Fear}, generating a type of negative prediction error (NPE) that is thought to facilitate extinction (*7, 17, 18*). We find that photosensitive dopamine

neurons that are either inhibited or activated by the CS_{Fear}+ are activated by omission of the US_{Fear} (shock) (**fig. S4A-F**), indicating that these neurons encode both an NPE and the salience of the omitted US_{Fear}. To determine whether precisely timed presentation of a CS_{Rew}+ at the offset of the CS_{Fear}+ could also facilitate extinction, mice were counter conditioned in a simple Pavlovian fear conditioning paradigm and presented with the CS_{Rew}+ or CS_{Rew}- at the offset of the CS_{Fear}+ and during extinction training (**Fig. 1E-G**). Mice presented with the CS_{Rew}+ at CS_{Fear+} offset displayed enhanced fear extinction and extinction memory recall that was not observed in mice presented with CS_{Rew}- at CS_{Fear+} offset or that had dopamine neurons inhibited during the presentation of the CS_{Rew}+, (**Fig. 1G,H** and **fig. S4G**). The timing of the CS_{Rew}+ presentation during the CS_{Fear}+ is critical for facilitating extinction, as a random presentation during the intertrial interval did not alter extinction training or extinction memory recall (**fig. S4H-J**).

The CeA and dopamine signaling in the CeA have emerged as an important for regulating discriminatory threat learning (*7, 19-22*). The dynamics of dopamine release in the CeA during either positive or negative reinforcement and how dopamine evoked by these distinct valances interact are not known. To establish the dynamics of dopamine release in the CeA during positive and negative reinforcement learning, and the impacts of a CS_{Rew}+ on dopamine release associated with the CS_{Fear}+ during threat conditioning, we monitored dopamine release in the CeA during reward and fear conditioning. To resolve dopamine dynamics under both generalized and discriminatory fear, we first determined whether generalized fear could be induced and then reversed by reconditioning with co-presentation of a CS_{Rew}+ that is dependent on the activation of dopamine neurons (**Fig. 2A** and **fig. S5A**). Mice were conditioned in a probabilistic conditioning paradigm to induce generalization, followed by two days of reconditioning with co-

presentation of the CS_{Rew}+ or CS_{Rew}- with the $CS_{0.7}$ (**Fig. 2A** and **fig. S5B**). All groups of mice showed generalized fear after a single conditioning session (**Fig. 2B**; ret1), but mice presented with the CS_{Rew}+ at the onset of the $CS_{0.7}$ during reconditioning displayed improved discrimination (**Fig. 2B** and **fig. S5C**; CS_{Rew}+; ret2,3). In contrast, mice presented with the CS_{Rew}- or had dopamine neurons inhibited by JAWS during the presentation of the CS_{Rew}+ displayed persistent generalized threat responses (**Fig. 2B**; CS_{Rew}- and JAWS- CS_{Rew}+; ret2,3).

Next, we confirmed that dopamine release could be detected in the CeA, DAT-Cre mice were injected with a virus to conditionally express the red-shifted stimulatory opsin Chrimson (*23*) (AAV-FLEX-Chrimson-tdTomato) in dopamine neurons in the VTA and a virus to express the dopamine sensor dLight1.3b (*24*) in the CeA (AAV-dLight1.3b). Stimulation of dopamine neurons evoked transient dopamine release in a frequency and stimulus duration-dependent manner (**fig. S5D-E**).

Finally, we monitored dopamine release during positive reinforcement learning and reward-induced reversal of fear generalization. During positive reinforcement learning, dopamine was initially not released in the CeA to the CS_{Rew}+ or CS_{Rew}- but was released in response to the US_{Rew} (**Fig. 2C-F** and **fig. S5F,G**). As learning progressed, dopamine signals emerged to the CS_{Rew}+ but not the CS_{Rew}- and responses to the US_{Rew} diminished (**Fig. 2C-F** and **fig. S5F,G**). During probabilistic fear conditioning (**fig. S5H,I**) dopamine release was initially detected in response to the $US_{0.3mA}$ (**Fig. 2G**; FC1). Co-presentation of the CS_{Rew}+ during reconditioning did not alter dopamine release to the fear $CS_{0.7}$ but significantly reduced dopamine release to the $CS_{0.3}$ (**Fig. 2G,H**; FC2 and FC3).

To determine whether VTA dopamine projections to the CeA are sufficient to facilitate the reversal of threat generalization, we expressed ChR2 (AAV-FLEX-ChR2) or control virus

mCherry (AAV-FLEX-mCherry) in VTA dopamine neurons (DAT-Cre mice) and implanted optical fibers over the CeA (**fig. S6A**). Fear conditioning with a high-intensity US (0.5 mA) induced generalized responses and stimulation of VTA dopamine terminals in the CeA (1s, 20 Hz) effectively reduced generalized fear responses with just a single reconditioning session (**fig. S6B-E**).

To establish whether dopamine terminal stimulation in the CeA is sufficient to reverse generalization under increased uncertainty, and whether the effect is dopamine dependent, we expressed ChR2 in VTA dopamine neurons and conditionally mutated the gene encoding tyrosine hydroxylase (*Th*), the rate limiting enzyme in dopamine production, using CRISPR/SaCas9 mutagenesis (**Fig. 3A,B** and **fig. S6F**) (*25*). Optical fibers were implanted over the CeA (**fig. S6F**) to deliver 1 s of dopamine terminal stimulations (20 Hz) at the onset of the high probability $CS_{0.7}$ during reconditioning (**Fig. 3C** and **fig. S6G**). Again, stimulation of dopamine terminals effectively induced discrimination between $CS_{0.7}$ and $CS_{0.3}$ that was dopamine dependent (**Fig. 3D,E**). Similarly, brief (1s) stimulation of dopamine terminals in the CeA at the offset of the CS_{Fear}+ and CS_{Fear}- (**Fig. 3F**) facilitated extinction and enhanced extinction memory recall in a dopamine-dependent manner (**Fig. 3G,H**).

To determine which dopamine receptors in the CeA are important for the ability of dopamine terminal stimulation to reverse threat generalization and enhance fear extinction, we generated CRISPR guides to selectively mutate the genes encoding D1 (sg*Drd1*) and D2 (sg*Drd2*) receptors in these cells, both of which are broadly expressed on subpopulations of inhibitory CeA GABA neurons (*22, 26-28*). DAT-Cre::VGAT-Flp double transgenic mice were injected with AAV-FLEX-ChR2-mCherry into the VTA and either AAV-FLEXfrt-SaCas9-U6-sg*Drd1*, AAV-FLEXfrt-SaCas9-U6-sg*Drd2* or AAV-FLEXfrt-SaCas9-U6-sg*Rosa26* (control)

into the CeA and an optical fiber was placed above the CeA (**fig. S7A,B**). Both the sg*Drd1* and sg*Drd2* CRISPRs resulted in significant reductions in mRNA levels in the CeA relative to the sg*Rosa26* control CRISPR (**Fig. 3I,J** and **fig. S7C**). Reconditioning in the probabilistic fear paradigm (**Fig. 3K** and **fig. S7D**) facilitated discrimination in the sg*Rosa26* and sg*Drd1* mice, but not in the sg*Drd2* mice (**Fig. 3L** and **fig. S7E**). Following fear conditioning, mice underwent extinction training with optical stimulation of dopamine terminals in the CeA (1s, 20Hz) at the offset of the $CS_{0.7}$ and $CS_{0.3}$ (**Fig. 3M**). The sg*Rosa26* control mice showed reduced freezing across the extinction session to both CSs (**Fig. 3N**). In contrast, the sg*Drd1* mice displayed reduced freezing from the onset of the extinction training (**Fig. 3N**) and sg*Drd2* mice showed persistent freezing across the extinction session (**Fig. 3N**), indicating that D1 and D2 receptor signaling have opposing actions during extinction training. During extinction recall, all mice showed similar freezing levels (**Fig. 3O**), suggesting that loss of D1 or D2 receptor signaling independently may affect the expression of the extinction responses during training but are not required for the consolidation of the extinction memory.

Subpopulations of genetically distinct CeA neurons are activated (Fear-On) or inhibited (Fear-Off) by conditioned threat stimuli and contribute to associative fear learning (*20, 21, 29-32*), but how these neurons respond during generalized fear or the impact of dopamine on this encoding is not known. To address this, DAT-Cre mice were injected with ChR2 and *Th*-CRISPR virus or *Rosa26* control virus in the VTA and implanted an optical fiber and recording electrodes in the CeA (**Fig. 4A** and **fig. S8A**). Stimulation of dopamine-releasing terminals (10 pulses at 20 Hz) in the CeA resulted in neuronal excitations and inhibitions (**Fig. 4B**). The proportion of neurons responsive to dopamine terminal stimulation was significantly reduced in mice with mutated *Th* (**Fig. 4B**). Within our control group (sg*Rosa26*) stimulation of dopamine

terminals (1s, 20 HZ) enhanced discriminatory fear following reconditioning (**Fig. 4D** and **fig. S8B,C**), as above. Within the CeA, a subset of neurons was phasically excited by both CSs during the pre-test phase (**Fig. 4E**), but no neurons were detected that were inhibited by either CS (**fig. S8D**). Following the first conditioning when mice displayed generalized freezing responses, we observed equivalent transient excitations and prolonged inhibitions (**Fig. 4E,F**; ret1). After reconditioning with dopamine terminal stimulation, we observed discriminatory freezing behavior that was associated with discriminatory encoding of the $CS_{0.7}$ and $CS_{0.3}$ by CeA neurons (**Fig. 4D,F**; ret2). In contrast to sg*Rosa26* control mice, reconditioning mice with *Th* mutagenesis in VTA dopamine neurons with dopamine terminal stimulation in the CeA did not promote discriminatory behavior (**Fig. 4G** and **fig. S8B,C**). During the pre-test and first retention test, CeA neurons from sg*Th* mice showed a similar response to the sg*Ros26* group (**Fig. 4H,I** and **fig. S8D**). However, sg*Th* mice had a significantly smaller proportion of inhibited neurons (**fig. S8D**), suggesting that inhibited responses may be mediated in part by dopamine signaling. Following reconditioning, equivalent responses to the $CS_{0.7}$ and $CS_{0.3}$ were observed, consistent with these mice displaying persistent generalized fear responses (**Fig. 4G,I**).

Following fear conditioning, mice underwent extinction training (**Fig. 4J** and **fig. S8E**). Half of the control mice received dopamine terminal stimulation at the offset of the $CS_{0.7}$ and $CS_{0.3}$ and half received no stimulation. All *Th* mutagenized mice received optical stimulation. CeA neurons responsive to the CS were significantly reduced following extinction in mice with dopamine terminal stimulation relative to non-stimulated controls and *Th* mutagenized mice (**Fig. 4J-M**), indicating that the enhanced extinction observed in the sg*Rosa26* mice that received dopamine terminal stimulation is associated with an enhanced loss of responsive CeA neurons.

Our results demonstrate that a stimulus associated with a positive outcome can serve as a potent modulator of fear learning through dopamine-dependent regulation of fear circuitry. We find that the effectiveness of a positive stimulus enhancing fear extinction is dependent on when the CS_{Rew}+ is presented, indicating that timing is critical. Mechanistically, we demonstrate that generalized fear responses are associated with non-discriminatory encoding in the CeA. Precisely timed transient increases in dopamine within the CeA can facilitate the reversal of generalized behavior and non-discriminatory encoding, and the same is true for the facilitation of extinction. In conclusion, stimuli associated with positive reinforcement are an effective means to modify threat encoding by CeA neurons and fear-related behavior. Thus, manipulating the salience encoding of dopamine, either naturally or artificially, has a potent influence over discriminatory fear learning and the extinction of fear memories.

References

1. X. L. Feng Biao, Z. Weixing, C. Ting, W. Wenqing, Z. Xifu, The inhibitive effect of positive emotions on fear generalization. *Acta Psychologica Sinica* **49**, 317-328 (2017).
2. T. D. Zbozinek, M. G. Craske, Positive affect predicts less reacquisition of fear: relevance for long-term outcomes of exposure therapy. *Cogn Emot* **31**, 712-725 (2017).
3. P. H. Janak, K. M. Tye, From circuits to behaviour in the amygdala. *Nature* **517**, 284-292 (2015).
4. P. Tovote, J. P. Fadok, A. Luthi, Neuronal circuits for fear and anxiety. *Nat Rev Neurosci* **16**, 317-331 (2015).
5. S. M. Warlow, K. C. Berridge, Incentive motivation: 'wanting' roles of central amygdala circuitry. *Behav Brain Res* **411**, 113376 (2021).
6. R. Hamati, J. Ahrens, C. Shvetz, M. R. Holahan, L. Tuominen, 65 years of research on dopamine's role in classical fear conditioning and extinction: A systematic review. *Eur J Neurosci* **59**, 1099-1140 (2024).
7. Y. S. Jo, G. Heymann, L. S. Zweifel, Dopamine Neurons Reflect the Uncertainty in Fear Generalization. *Neuron* **100**, 916-925 e913 (2018).
8. E. E. Steinberg *et al.*, Amygdala-Midbrain Connections Modulate Appetitive and Aversive Learning. *Neuron* **106**, 1026-1043 e1029 (2020).
9. E. Casey, M. E. Avale, A. Kravitz, M. Rubinstein, Dopaminergic innervation at the central nucleus of the amygdala reveals distinct topographically segregated regions. *Brain Struct Funct* **228**, 663-675 (2023).

10. M. Watabe-Uchida, L. Zhu, S. K. Ogawa, A. Vamanrao, N. Uchida, Whole-brain mapping of direct inputs to midbrain dopamine neurons. *Neuron* **74**, 858-873 (2012).
11. W. Schultz, P. Dayan, P. R. Montague, A neural substrate of prediction and reward. *Science* **275**, 1593-1599 (1997).
12. B. B. Gore, M. E. Soden, L. S. Zweifel, Visualization of plasticity in fear-evoked calcium signals in midbrain dopamine neurons. *Learn Mem* **21**, 575-579 (2014).
13. A. S. Chuong *et al.*, Noninvasive optical inhibition with a red-shifted microbial rhodopsin. *Nat Neurosci* **17**, 1123-1129 (2014).
14. L. Fellinger *et al.*, A midbrain dynorphin circuit promotes threat generalization. *Curr Biol* **31**, 4388-4396 e4385 (2021).
15. S. S. Correia, A. G. McGrath, A. Lee, A. M. Graybiel, K. A. Goosens, Amygdala-ventral striatum circuit activation decreases long-term fear. *Elife* **5**, (2016).
16. K. J. Ressler *et al.*, Post-traumatic stress disorder: clinical and translational neuroscience from cells to circuits. *Nat Rev Neurol* **18**, 273-288 (2022).
17. L. X. Cai *et al.*, Distinct signals in medial and lateral VTA dopamine neurons modulate fear extinction at different times. *Elife* **9**, (2020).
18. X. I. Salinas-Hernandez *et al.*, Dopamine neurons drive fear extinction learning by signaling the omission of expected aversive outcomes. *Elife* **7**, (2018).
19. P. Botta *et al.*, Regulating anxiety with extrasynaptic inhibition. *Nat Neurosci* **18**, 1493-1500 (2015).
20. S. Ciocchi *et al.*, Encoding of conditioned fear in central amygdala inhibitory circuits. *Nature* **468**, 277-282 (2010).
21. C. A. Sanford *et al.*, A Central Amygdala CRF Circuit Facilitates Learning about Weak Threats. *Neuron* **93**, 164-178 (2017).
22. D. De Bundel *et al.*, Dopamine D2 receptors gate generalization of conditioned threat responses through mTORC1 signaling in the extended amygdala. *Mol Psychiatry* **21**, 1545-1553 (2016).
23. N. C. Klapoetke *et al.*, Independent optical excitation of distinct neural populations. *Nat Methods* **11**, 338-346 (2014).
24. T. Patriarchi *et al.*, Ultrafast neuronal imaging of dopamine dynamics with designed genetically encoded sensors. *Science* **360**, (2018).
25. A. C. Hunker *et al.*, Conditional Single Vector CRISPR/SaCas9 Viruses for Efficient Mutagenesis in the Adult Mouse Nervous System. *Cell Rep* **30**, 4303-4316 e4306 (2020).
26. J. Kim, X. Zhang, S. Muralidhar, S. A. LeBlanc, S. Tonegawa, Basolateral to Central Amygdala Neural Circuits for Appetitive Behaviors. *Neuron* **93**, 1464-1479 e1465 (2017).
27. K. M. McCullough, N. P. Daskalakis, G. Gafford, F. G. Morrison, K. J. Ressler, Cell-type-specific interrogation of CeA Drd2 neurons to identify targets for pharmacological modulation of fear extinction. *Transl Psychiatry* **8**, 164 (2018).
28. K. M. McCullough, F. G. Morrison, J. Hartmann, W. A. Carlezon, Jr., K. J. Ressler, Quantified Coexpression Analysis of Central Amygdala Subpopulations. *eNeuro* **5**, (2018).
29. S. Duvarci, D. Popa, D. Pare, Central amygdala activity during fear conditioning. *J Neurosci* **31**, 289-294 (2011).
30. J. P. Fadok *et al.*, A competitive inhibitory circuit for selection of active and passive fear responses. *Nature* **542**, 96-100 (2017).
31. W. Haubensak *et al.*, Genetic dissection of an amygdala microcircuit that gates conditioned fear. *Nature* **468**, 270-276 (2010).
32. H. Li *et al.*, Experience-dependent modification of a central amygdala fear circuit. *Nat Neurosci* **16**, 332-339 (2013).

33. B. B. Gore, M. E. Soden, L. S. Zweifel, Manipulating gene expression in projection-specific neuronal populations using combinatorial viral approaches. *Curr Protoc Neurosci* **65**, 4 35 31-20 (2013).

Figures and legends

Figure 1

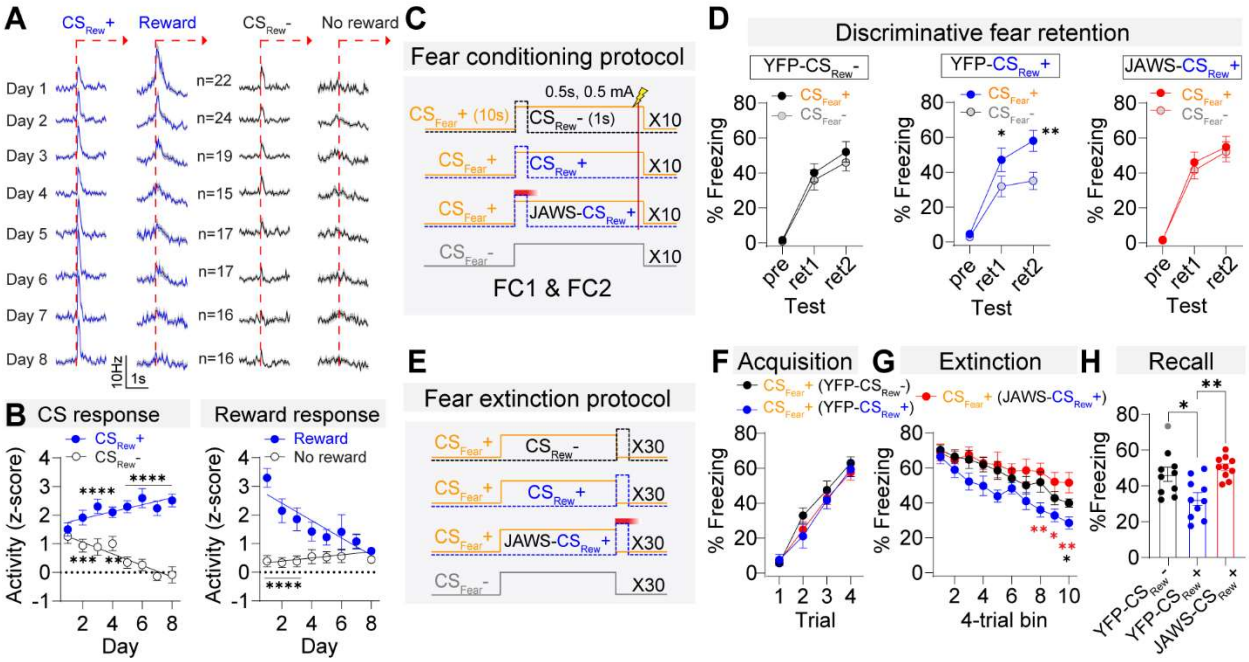

Figure 1. Impact of CS_{Rew}+ evoked dopamine on discriminatory fear and fear extinction. (**A**) Average dopaminergic responses to CSs and head entries for reward consumption (total 146 cells from 7 mice). (**B**) Normalized responses to CS_{Rew}+, CS_{Rew}-, and reward retrieval (relative to baseline firing before each CS). CS_{Rew}+ and CS_{Rew}- responses were positively and negatively correlated with training days, respectively (Pearson's correlation, CS_{Rew}+, $r = 0.26$, $P = 0.002$ and negatively CS_{Rew}-, $r = -0.43$, $P < 0.001$). Reward responses were negatively correlated in CS_{Rew}+ trials ($r = -0.4$, $P < 0.001$). Significant differences between CS_{Rew}+ and CS_{Rew}-, and Reward versus No reward following the CS_{Rew}- were observed (**$P < 0.01$, ***$P < 0.001$, ****$P < 0.0001$). (**C**) Schematic of timing sequences for CS_{Rew}+ and CS_{Rew}- presentations and

JAWS-mediated inhibition during fear conditioning (CS_{Rew}+ = 10 mice, CS_{Rew}- = 10 mice, and JAWS- CS_{Rew}+ = 10 mice). (**D**) Freezing responses to the CS_{Fear}+ and CS_{Fear}- during the pre-test and retention tests 1 and 2. CS_{Rew}+ mice showed significant discriminatory freezing (*$P < 0.05$, **$P < 0.01$). (**E**) Schematic of simple Pavlovian fear conditioning and extinction paradigm with precise timing of CS_{Rew}+, CS_{Rew}-, and JAWS inhibition during extinction training. (**F**) Fear acquisition in all three groups. (**G**) Fear extinction training in all three groups showing enhanced extinction in the YFP-CS_{Rew}+ group (*$P < 0.05$, **$P < 0.01$). (**H**) Extinction memory recall showing enhanced recall in the YFP-CS_{Rew}+ group (*$P < 0.05$, **$P < 0.01$). All data presented as mean ± S.E.M.

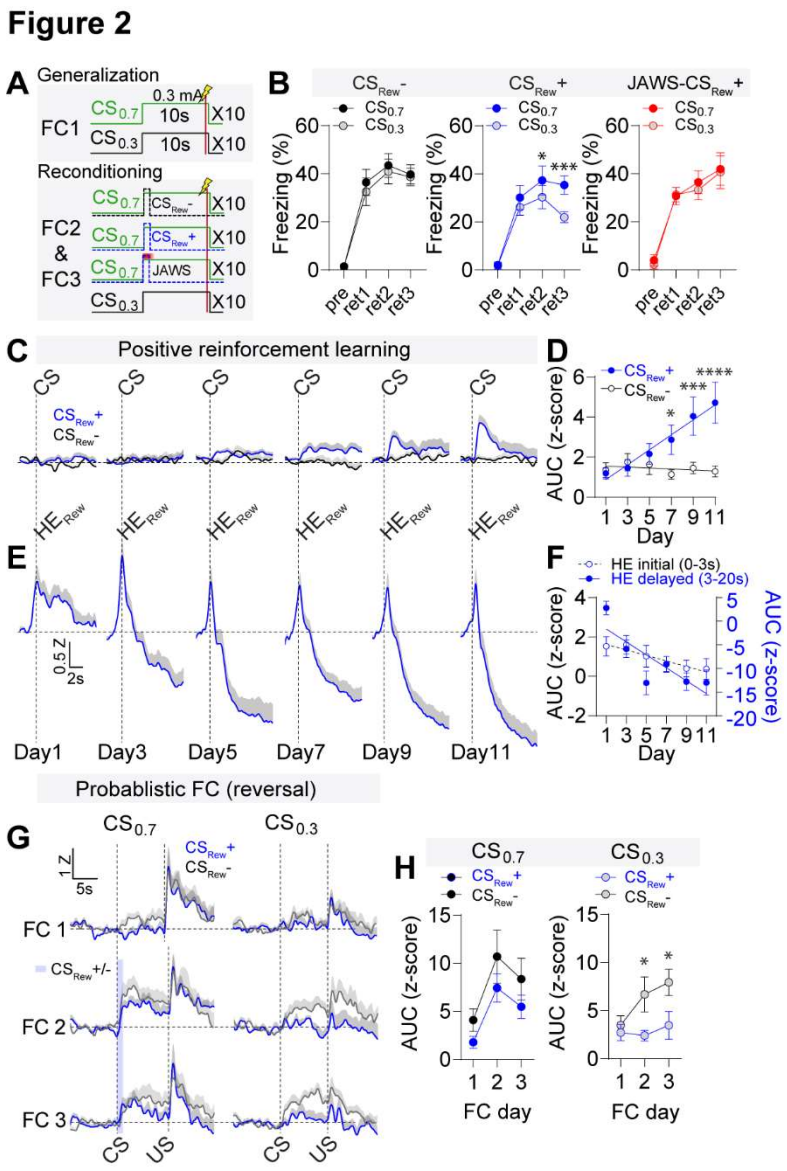

Figure 2. Impact of CS_{Rew}+ on fear-evoked dopamine in the CeA. (**A**) Schematic of probabilistic fear conditioning paradigm to induce fear generalization and CS_{Rew}+ reversal (CS_{Rew}- = 10 mice, CS_{Rew}+ = 10 mice, and JAWS- CS_{Rew}+ = 10 mice). (**B**) Following the induction of a generalized threat response, reconditioning with the CS_{Rew}+ facilitated discrimination between the $CS_{0.7}$ and $CS_{0.3}$ that was not observed with co-presentation of the CS_{Rew}- or when dopamine neurons were inhibited by JAWS during the CS_{Rew}+ presentation (**P* < 0.05, ****P* < 0.001). (**C**) Average traces showing increased dopamine release in the CeA

during positive reinforcement learning to the CS_{Rew}+ but not to the CS_{Rew}-. (**D**) Average AUC for CS_{Rew}+ and CS_{Rew}- (*$P < 0.05$, ***$P < 0.001$, ****$P < 0.001$, CS_{Rew}- = 9 mice, CS_{Rew}+ = 10 mice). (**E**) Averaged CeA dopamine signals in response to head entry for reward retrieval (HE_{Rew}). (**F**) AUC during head entry for reward retrieval segregated into the initial response (0-3s, $R^2 = 0.04941$, $P = 0.0147$) and secondary response (3-20s, $R^2 = 0.1953$, $P < 0.0001$). (**G**) Dopamine signal in the CeA during fear conditioning with the $CS_{0.7}$ and $CS_{0.3}$ (FC1) and during reconditioning with the CS_{Rew}+ or CS_{Rew}- (FC2 and FC3). (**H**) Mean area under the curve (AUC) of the z-scored dopamine signals in the CeA to the $CS_{0.7}$ and $CS_{0.3}$ during fear conditioning and reconditioning. Co-presentation of the CS_{Rew}+ prevented the increase in dopamine release in the CeA in response to the $CS_{0.3}$ (*$P < 0.05$). All data presented as mean ± S.E.M.

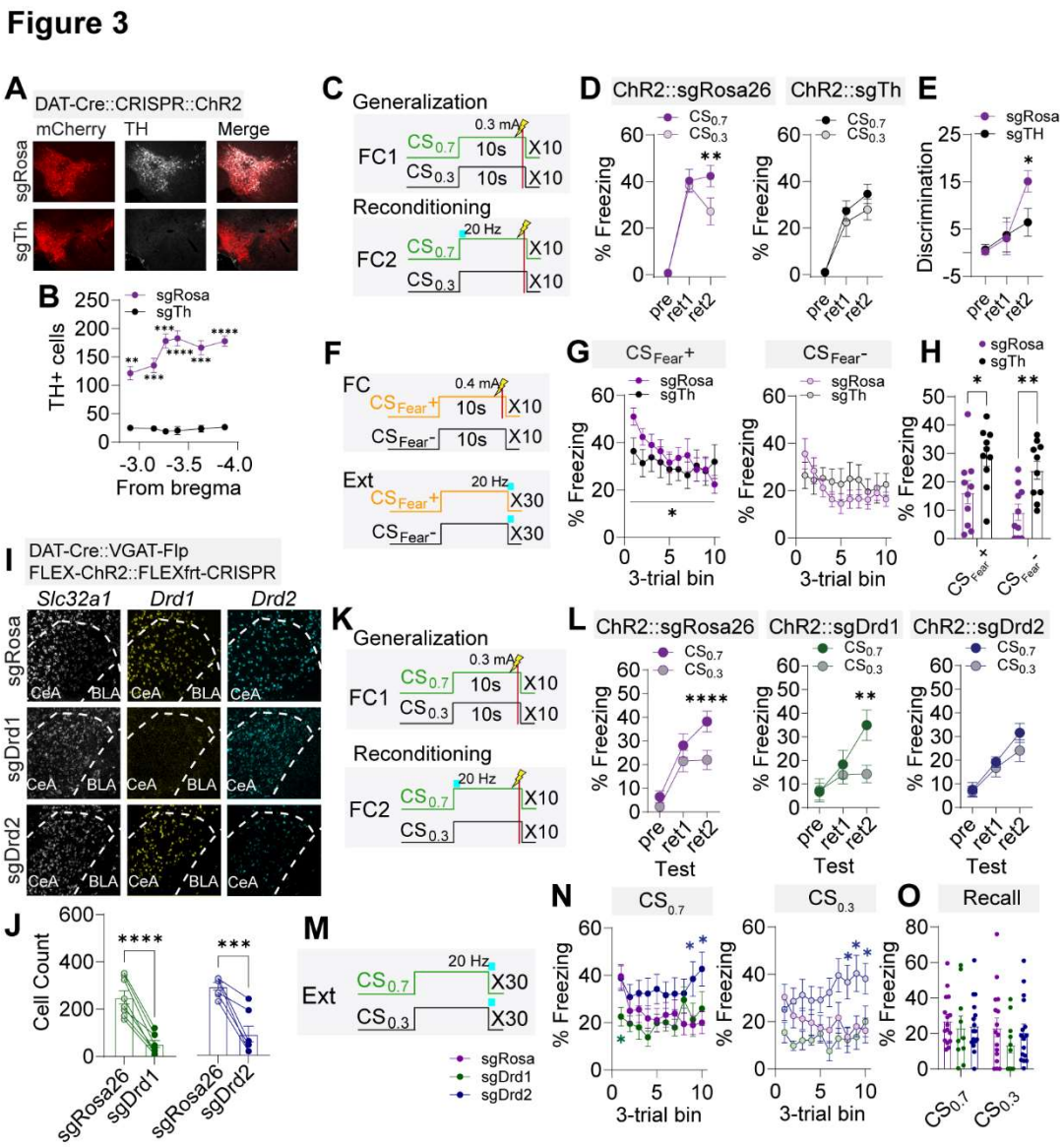

Figure 3. Dopamine release in the CeA is critical for reversing generalization and facilitating extinction. (**A**) Histological validation of *Th* inactivation. (**B**) Quantitative analysis of reduced TH levels in the VTA of sg*Rosa26* control (N = 6) and sg*Th* (N = 5) mice (***P* < 0.01, ****P* < 0.001, *****P* < 0.001, 6 sections/mice). (**C**) Schematic of probabilistic fear conditioning paradigm and optogenetic stimulation during reconditioning. (**D**) Following the induction of a generalized threat response, reconditioning with the optical stimulation of dopamine terminals for 1s facilitated discrimination between the $CS_{0.7}$ and $CS_{0.3}$ that was not

observed in *Th* mutagenized mice (**$P < 0.01$; sg*Rosa26* = 10 mice and sg*Th* = 10 mice). (**E**) Comparison of fear discrimination between groups (*$P < 0.05$). (**F**) Schematic of simple Pavlovian fear conditioning and extinction paradigm with precise timing of optical stimulation of dopamine terminals in the CeA during extinction training (sg*Rosa26* = 10 mice and sg*Th* = 10 mice). (**G**) Fear extinction training in both groups showing enhanced extinction in the sg*Rosa26* stimulated mice (*$P < 0.05$). (**H**) Extinction memory recall showing enhanced recall in the sg*Rosa26* stimulated mice (*$P < 0.05$, **$P < 0.01$). (**I**) RNAscope validation of *Drd1* and *Drd2* mRNA levels in the CeA following mutagenesis. (**J**) Quantitative of reduced mRNA levels associated with nonsense mediated mRNA decay following CRISPR mutagenesis (***$P < 0.001$, ****$P < 0.0001$; sg*Rosa26*/sg*Drd1* = 8 sections from 4 mice and sg*Rosa26*/sg*Drd2* = 7 sections from 4 mice). (**K**) Schematic of probabilistic fear conditioning paradigm and optogenetic stimulation during reconditioning (sg*Rosa26* = 15 mice, sg*Drd1* = 10 mice, and sg*Drd2* =16 mice). (**L**) Following the induction of a generalized threat response, reconditioning with the optical stimulation of dopamine terminals for 1s facilitated discrimination between the $CS_{0.7}$ and $CS_{0.3}$ in sg*Rosa26* and sg*Drd1* mice that was not observed in *Drd2* mutagenized mice (**$P < 0.01$, ****$P < 0.0001$). (**M**) Schematic of extinction paradigm with precise timing of optical stimulation of dopamine terminals in the CeA during extinction training. (**N**) During fear extinction training, freezing to the $CS_{0.7}$ and $CS_{0.3}$ was reduced early in sg*Drd1* mice and increased late in sg*Drd2* mice relative to sg*Rosa26* control mice (*$P < 0.05$). (**O**) Freezing during extinction memory recall was not different between groups. All data presented as mean ± S.E.M.

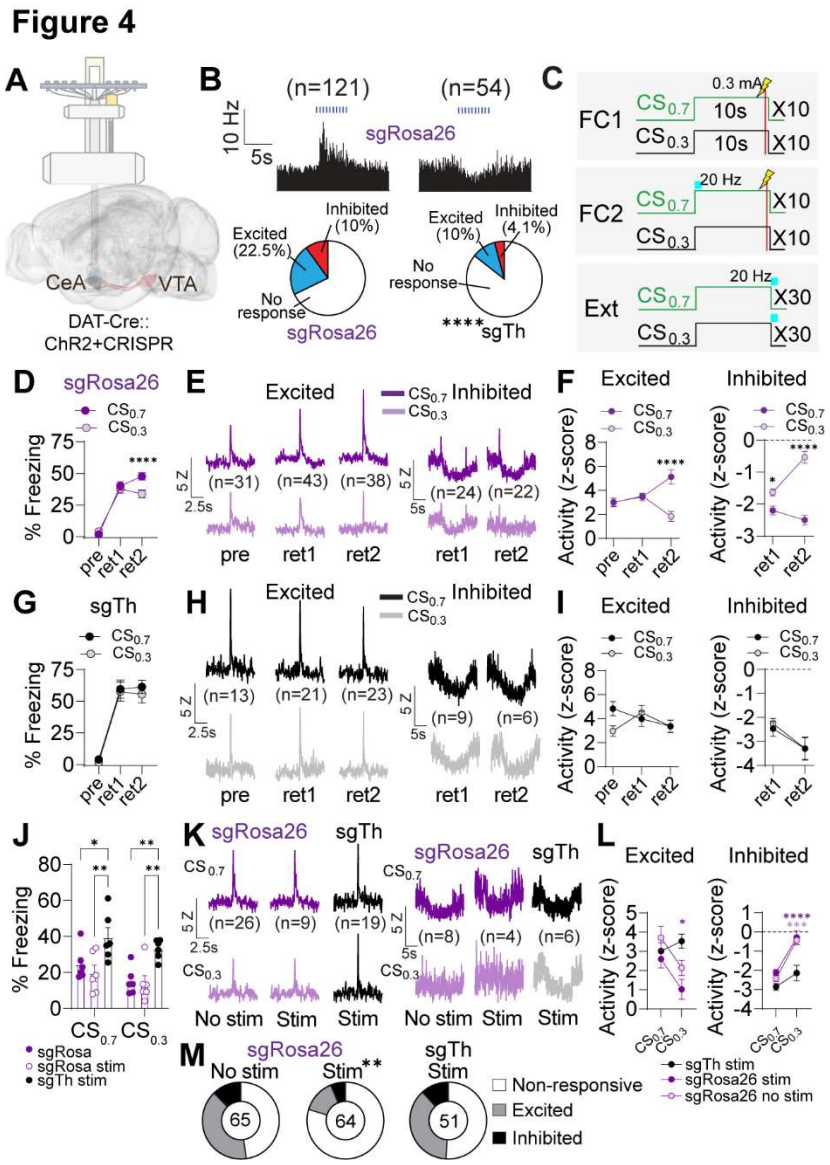

Figure 4. Dopamine regulates discriminatory fear encoding in the CeA. (**A**) Schematic of AAV-FLEX-ChR2-mCherry and AAV-FLEX-SaCas9-u6-sg*Th* injected into the VTA of DAT-Cre mice and optrode implant for analysis of dopamine neuron activity. (**B**) Responses of CeA neurons to dopamine terminal stimulation showing reduced excitatory and inhibitory responses in sg*Th* compared to sg*Rosa26* mice (Fisher's exact test, ****$P < 0.0001$, sg*Rosa26* = 405 cells from 12 mice and sg*Th* = 233 cells from12 mice). (**C**) Schematic of probabilistic fear conditioning paradigm (FC1) and optogenetic stimulation during reconditioning (FC2) and

extinction (Ext). (**D**) Freezing to the $CS_{0.7}$ and $CS_{0.3}$ in sg*Rosa26* mice with CeA recordings during pre-conditioning test, retention test 1, and retention test 2 (****$P < 0.0001$; sg*Rosa26* = 12 mice). (**E**) Average firing to $CS_{0.7}$ and $CS_{0.3}$ in sg*Rosa26* mice during pre-conditioning test, retention test 1, and retention test 2. (**F**) Normalized responses to $CS_{0.7}$ and $CS_{0.3}$ (relative to baseline firing before each CS) in sg*Rosa26* mice. During pre-conditioning test and retention test 1, there was no discriminatory encoding in excited cells. Following reconditioning with dopamine terminal stimulation, discriminatory encoding was significantly enhanced (*$P < 0.05$, ****$P < 0.0001$). In inhibited cells, a small but significant discrimination between the encoding of the $CS_{0.7}$ and $CS_{0.3}$ was observed during retention test 1, but this was greatly enhanced following reconditioning with dopamine terminal stimulation (Two-way ANOVA). (**G**) Freezing to the $CS_{0.7}$ and $CS_{0.3}$ in sg*Th* mice with CeA recordings during pre-conditioning test, retention test 1, and retention test 2 (sg*Th* = 6 mice). (**H**) Average firing to $CS_{0.7}$ and $CS_{0.3}$ in sg*Th* mice during pre-conditioning test, retention test 1, and retention test 2. (**I**) Normalized responses to $CS_{0.7}$ and $CS_{0.3}$ (relative to baseline firing before each CS) in sg*Th* mice. During pre-test, retention test 1 and retention test 2, there was no discriminatory encoding in excited cells. In inhibited cells, no discrimination between the encoding of the $CS_{0.7}$ and $CS_{0.3}$ was observed during retention test 1 or retention test 2. (**J**) Freezing to the $CS_{0.7}$ and $CS_{0.3}$ during extinction recall with CeA recordings in sg*Rosa26* mice with and without dopamine terminal stimulation and in sg*Th* mice with dopamine terminal stimulation during extinction training (*$P < 0.05$, **$P < 0.01$; sg*Rosa26* = 6 mice, sg*Rosa26* stim = 6 mice and sg*Th* stim = 6 mice). (**K**) Average firing to $CS_{0.7}$ and $CS_{0.3}$ in all groups during extinction recall. (**L**) Normalized responses to $CS_{0.7}$ and $CS_{0.3}$ (relative to baseline firing before each CS) in all groups during extinction recall. There were no differences detected in the excited cells in response to the $CS_{0.7}$, but significant

differences were observed in response to the $CS_{0.3}$ (*$P < 0.05$, ***$P < 0.001$, ****$P < 0.0001$). (**M**) The proportion of cells either excited or inhibited by the CSs during extinction recall was significantly reduced in the sg*Rosa26* mice with dopamine terminal stimulation during extinction training compared to sg*Rosa26* mice without dopamine terminal stimulation and sg*Th* mice with dopamine terminal stimulation (Fisher's exact test, **$P < 0.01$). All data presented as mean ± S.E.M.

Methods

Animals

Male and female mice aged 2-6 months, including *Slc6a3*$^{Cre+}$ (DAT-Cre) mice and double transgenic mice *Slc6a3*$^{cre+}$::*Slc32a1*$^{Flp+}$ (DAT-Cre::VGAT-Flp), were housed on a 12/12 h light/dark cycle (lights on at 7 am) with free access to food and water. Mice were randomly assigned into groups and experiments were conducted during the light cycle. All procedures were performed in compliance with the guidelines set forth by the Institutional Animal Care and Use Committee.

Virus production and surgery

All AAV vectors were internally produced (final titer, 1-3 x 10^{12} particles/ml) following previously outlined protocols (*33*). Cre-dependent optogenetics viruses included AAV1-FLEX-JAWS-EGFP, AAV1-FLEX-ChR2-mCherry, and AAV1-FLEX-Chrimson-tdTomato and AAV1-FLEX-EYFP (control). The dopamine sensor virus was AAV1-CAG-dLight1.3b. Cre-dependent CRISPR viruses were AAV1-FLEX-SaCas9-HA-U6-sg*Th* and AAV1- FLEX-SaCas9-HA-U6-sg*Rosa26* (control). Flp-dependent CRISPR viruses were AAV1-FLEXfrt-SaCas9-HA-U6-sg*Drd1*, AAV1-FLEXfrt-SaCas9-HA-U6-sg*Drd2,* and AAV1-FLEXfrt-SaCas9-HA-U6-sg*Rosa26* (control). Viral vectors were stored at -80°C before surgery. On the day of

surgery, mice were anesthetized under isoflurane (1-4%) and head fixed in a stereotaxic frame. One of the viral vectors (0.5 µl) was bilaterally or unilaterally injected into the VTA (3.3 mm posterior, 0.5 mm lateral, and 4.5 mm ventral to bregma) or CeA (1.2 mm posterior, 2.9 mm lateral, and 4.6 mm ventral to bregma) at a rate of 0.25 µl/min. Then optic fibers (200 µm inner core, 0.22 NA) and/or a photometry fiber (400 µm fiber, 0.66 NA and 1.25 mm diameter, Doric Lenses) were bilaterally (optic fibers) or unilaterally (fiber photometry fiber; right hemisphere) implanted dorsal to the VTA (4.0 mm ventral to bregma) or CeA (4.2 mm ventral to bregma). The fibers were secured in place with two anchoring screws and dental cement. For single-unit recording, a microdrive containing 4 tetrodes (25 µm diameter tungsten wire; California Fine Wire) and an optic fiber was implanted dorsal to the VTA (3.7 mm to the brain surface) or CeA (3.8 mm to the brain surface). Tetrodes were cut and gold-plated to reach impedances of 100-300 kΩ tested at 1 kHz. The distance between the fiber and tetrode tips was about 500 µm.

Pavlovian reinforcement learning

Mice were calorie-restricted to 85% of their baseline body weight. Each mouse was placed in one of four identical operant boxes (ENV-307W; Med Associates) with a food hopper on one wall, a speaker on the opposite wall, and a smooth plastic panel on the floor. There were 25 rewarding CSs and 25 non-rewarding CSs (CS_{Rew}+ and CS_{Rew}-; 8 kHz or 15 kHz tone, counterbalanced) trials per day with an average intertrial interval (ITI) of 2 min. The two CSs were presented in a random order. Each CS lasted for 10 s, and only CS_{Rew}+ was paired with a 20-mg food pellet (Bio-Serv). As a dependent variable, the number of head entries during the presentation of two CSs was measured using an infrared detector located in the food hopper.

Fear conditioning and extinction

Fear conditioning protocols consisted of three tone tests and two conditioning sessions on three consecutive days: pre-conditioning test (pre) in the morning and first fear conditioning in the afternoon on day 1 (FC1), post-conditioning retention test 1 (ret1) and second fear conditioning on day 2 (FC2), and post-conditioning retention test 2 (ret2) on day 3. Standard conditioning sessions were conducted in two identical chambers (ENV-307W; Med Associates), which were located in a different room from where Pavlovian reinforcement learning had been carried out. Each chamber was equipped with two speakers on the opposite walls and 24 shock grids on the floor. A petri dish filled with a 1% acetic acid solution was located under the shock grids (Context B). Animals were placed in the chambers and habituated for 2 min. Then two auditory CSs (CS_{Fear}+ and CS_{Fear}-; 4 kHz or 12 kHz, counterbalanced) were presented 10 times each in a pseudo-random order with an ITI of 60 s (CS_{Fear}+ was always presented on the first trial). CS_{Fear}+ (10 s) co-terminated with a 0.5 s footshock (US; 0.3-0.5 mA), but CS_{Fear}- (10 s) did not. For the reversal of fear generalization, the four-day paradigm was used: pre and FC1 on day 1 for generalization, ret1 and FC2 on day 2, ret2 and FC3 on day 3, and ret3 on day 4. During FC2 and FC3, either CS_{Rew}+ or CS_{Rew}- was presented together at the onset of CS_{Fear}+ as a compound cue for 1 s to noninvasively activate dopamine neurons. In a separate group, CS_{Rew}+ coincided with a continuous red light (640 nm, 5-10 mW, 1-s on followed by 1-s ramp down, LaserGlow) to inhibit JAWS-expressing neurons in the VTA. The chambers were cleaned between animals with the acetic acid solution. To measure fearful responses to both CSs, tone tests were performed in a different environment where white plastic inserts covered the walls and shock grids (context A). Mice were habituated in the inserts for 2 min, and then three CS_{Fear}+ and CS_{Fear}- trials were presented. For the extinction training, thirty CS_{Fear}+ and CS_{Fear}- each were delivered in context A. The inserts were wiped with 70% ethanol between animals.

In a probabilistic fear conditioning paradigm, all procedures were the same except for the probability of pairing between CS and US during conditioning sessions. Out of ten sets of alternating $CS_{0.7}$ and $CS_{0.3}$ trials (either 4 kHz or 12 kHz, counterbalanced), seven sets of $CS_{0.7}$ (10 s) were paired with 0.3 mA footshock US in a pseudo-random order. In the other three sets, $CS_{0.3}$ (10 s), but not $CS_{0.7}$, was paired with the footshock US to increase the uncertainty of US prediction (**fig. S3A**). The first set was always assigned as $CS_{0.7}$ -paired and $CS_{0.3}$-unpaired with the US.

To stimulate ChR2-expressing VTA neurons during fear conditioning and extinction training, a pulsed blue light (20 Hz, 473 nm, 1 s, LaserGlow) was delivered at the onset of the $CS_{0.7}$ (probabilistic conditioning) or at the offset of CS_{Fear}+ and CS_{Fear}- (extinction).

During the tests and conditioning sessions behavior was recorded via a video camera mounted on the ceiling. Movement velocities were calculated using tracking software (Ethovision XT 15, Noldus Technology). Freezing behavior was scored during the presentation of CSs if velocities were less than 0.75 cm/s for at least 1 s. The freezing criterion was determined based on the comparison between automatic and manual scoring using a sample dataset.

Single-unit recording

Individual calorie-restricted mice (85% baseline body weight) were placed in a holding cage, and their microdrive was connected to a preamplifier, which transferred neural data to a digital Lynx acquisition system (4SX, Neuralynx). Spiking signals from the tetrodes were amplified, filtered, and digitized at 32 kHz. Unit spikes were recorded for 1 ms when voltage potentials exceeded a predetermined threshold. To identify ChR2-expressing dopamine neurons, 10 blue light pulses (473 nm; 5 ms at 20 Hz) were presented 20 times via the optic fiber of the microdrive. The light

intensity was adjusted (5-15 mW/mm^2) to match light-evoked waveforms and spontaneous ones. Once light-responsive units were found, mice underwent 8 daily recording sessions from the following day. In each session, neuronal basal firing patterns were first measured for 10 min in the holding cage. Then, their firing responses were recorded when mice were engaged in Pavlovian reinforcement learning or fear conditioning test days. After the daily training, mice were transferred back to the holding cage, and 10 light pulses were delivered 20 times. If light-responsive units were not found, all tetrodes were lowered in 80 µm increments until light-responsive units were encountered.

Fiber photometry

Calorie-restricted mice were connected to fiber photometry patch cords (Doric Lenses) to record fluorescent dopamine signals (dLight1.3b) from the CeA. The dopamine sensor signals were recorded using RZ5 BioAmp Processor and Synapse software (Tucker Davis Technologies) with a 465 nm LED (531 Hz, sinusoidal, excitation, Doric Lenses) and 405 nm LED (211 Hz, sinusoidal, isosbestic, Doric Lenses). A sampling rate was set at 1,017.25 Hz. The LED intensity was calibrated at the tip of the optic fiber and maintained within the range of 30–40 µW. During behavioral experiments, Med Associates delivered TTL signals associated with CS deliveries and head entries for offline analysis. Dopamine signals were normalized to the baseline (10 s before CSs), and peri-CS activity was computed with a custom script (PEP developed by Dr. Scott Ng-Evans). To validate dopamine release in the CeA by stimulation of the VTA, an optic fiber implanted in the VTA was connected to red light (640 nm, 5 mW, 5 ms pulses, LaserGlow). Stimulation-evoked dopamine signals were recorded in response to diverse light parameters (5, 10, 20, and 40 Hz with 1 s or 3 s duration; 1 min interval, pseudo-random order).

In situ hybridization

DAT-Cre::VGAT-Flp male and female mice (9 weeks old) were used to validate CRISPR mutagenesis in the CeA using RNAScope (ACDBio RNAscope Multiplex Fluorescent V2). The animals were injected with either Flp-dependent sgRNA targeting Drd1 or Drd2 in the left CeA and Rosa26 (control) in the right CeA. After 5 weeks, mice were rapidly decapitated, and brains were promptly flash-frozen on dry ice to be stored at −80°C. CeA sections were collected and processed, keeping track of the right and left hemispheres (25 µm, coronal). Representative sections where the CRISPR virus was injected in the CeA were selected for hybridization (AP: −0.83 to -1.67 mm). RNAscope was carried out according to the direction of ACDBio V2 and probes for Vgat, Drd1/Drd2 and Cas9 from ACDBio were used to stain for the respective genes. Slides were coverslipped with Fluoromount with 4′,6-diamidino-2-phenylindole (DAPI) (Southern Biotech) and imaged using a confocal fluorescent microscope (University of Washington Keck Center, Leica SP8X confocal). Images for each slide were collected and analyzed using the same settings for consistency across the same brain slices. Quantification analysis was performed using ImageJ and Qpath 0.4.4 (QuPath).

Immunohistochemistry

After the completion of behavioral experiments, mice were euthanized and transcardially perfused with phosphate-buffered saline (PBS) and 4% paraformaldehyde. Brains were extracted and cryoprotected in 30% sucrose in PBS. To confirm virus expression and fiber/electrode placements, frozen brains were sectioned and stained overnight (30 µm for single-unit recording and 50 µm for optogenetics and fiber photometry). The following primary antibodies were used: Rabbit anti-tyrosin hydroxylase (1:1000; Millipore: AB152), Mouse anti-GFP (1:1000; Millipore: MAB3580), Rat anti-mCherry (1:1000; Invitrogen M11217), and Rabbit anti-HA (1:1000; Sigma H6908). Secondary antibodies were used with 1:200 dilution (Jackson

ImmunoResearch). Using a Nikon upright microscope and Keyence BZ-X710, images were collected to examine recording sites, fiber placements, and protein expression levels.

Quantification and statistical analysis

Single units recorded from the VTA were isolated based on various waveform features using Offline Sorter (Plexon). Only units displaying stable spikes throughout the recording session were further analyzed using Matlab software (MathWorks). To identify dopamine neurons, a cluster analysis was performed based on spike latency (≤ 8 ms) and probability (≥ 0.8) in response to light pulses. The cluster showing high light responsiveness and a high correlation between spontaneous and light-evoked waveforms was considered as dopaminergic. To examine dopamine neuronal activity during Pavlovian reinforcement learning, peri-event time histograms (PETHs; 50 ms bins) were constructed around the time of CSs and rewards. A reward event in each trial was defined as the first head entry into the food hopper after the food delivery. Firing rates in PETHs were transformed to z-scores relative to the pre-CS baseline firing (2.5 s epoch before CS onset). Average dopamine responses to CSs and rewards were measured during the 400 ms window from the onset of each event.

Statistical significance of all data was assessed using Prism software (GrapchPad Prism 10). See Extended Data Table 1 for detailed information about statistical results. Statistical tests for electrophysiological and behavioral results were performed with one-way ANOVAs across groups as well as mixed-design ANOVAs that contained within-subjects factors (e.g., CS and day) and between-subject variables (e.g., group). Once significant interactions were found, suitable post-hoc tests were used to confirm the statistical significance. Pearson's correlation tests were conducted to establish a relationship between two variables. Two-tailed P values <

0.05 were considered statistically significant. All data were tested for normality and represented as mean ± SEM.

Acknowledgments: Supported by National Institutes of Health grants R01DA044315(LSZ), R01MH135538 (LSZ), F32MH127801 (MSK) and National Research Foundation of Korea grant 2022M3E5E8017804 (YSJ). This work was also supported by the University of Washington Center of Excellence in Opioid Addiction Research (P30 DA048736). We thank Dr. James Allen, Dr. Avery Hunker, and Selena Schattauer for assistance with viral production and CRISPR construct design. We thank Dr. Scott Ng-Evans for assistance with photometry analysis. We also thank members of the Zweifel lab for their thoughtful discussion.

Author contributions: Y.S.J. and L.S.Z conceptualized the study. M.S.K, Y.S.J., and L.S.Z designed experiments. M.S.K., Y.S.J., G.H.P. and E.S. performed all experiments and collected and analyzed data. M.S.K., Y.S.J. and L.S.Z wrote the paper.

The authors have no competing interests to declare.

Correspondence and requests for materials should be addressed to Y.S.J or L.S.Z**:** larryz@uw.edu and ysjo@korea.ac.kr

Data availability: All data associated with this study will be made available upon acceptance of the manuscript.

Code availability: Code for fiber photometry analysis was derived from a publicly available source (Tucker Davis Technologies). Code for electrophysiology analysis was generated in house. All code will be available through GitHub (https://github.com/zweifellab/ephys).